

1

AD-A167 110

REPORT DOCUMENTATION PAGE		READ INSTRUCTIONS BEFORE COMPLETING FORM
1. REPORT NUMBER AFIT/CI/NR 86-62T	2. GOVT ACCESSION NO.	3. RECIPIENT'S CATALOG NUMBER
4. TITLE (and Subtitle) New Non-Linear FM Pulse-Compression Technique for Radar Applications		5. TYPE OF REPORT & PERIOD COVERED THESIS/DISSERTATION
		6. PERFORMING ORG. REPORT NUMBER
7. AUTHOR(s) Ronald A. Booher		8. CONTRACT OR GRANT NUMBER(s)
9. PERFORMING ORGANIZATION NAME AND ADDRESS AFIT STUDENT AT: University of Central Florida		10. PROGRAM ELEMENT, PROJECT, TASK AREA & WORK UNIT NUMBERS
11. CONTROLLING OFFICE NAME AND ADDRESS AFIT/NR WPAFB OH 45433-6583		12. REPORT DATE 1985
		13. NUMBER OF PAGES 50
14. MONITORING AGENCY NAME & ADDRESS (if different from Controlling Office)		15. SECURITY CLASS. (of this report) UNCLASS
		15a. DECLASSIFICATION/DOWNGRADING SCHEDULE
16. DISTRIBUTION STATEMENT (of this Report) APPROVED FOR PUBLIC RELEASE; DISTRIBUTION UNLIMITED		
17. DISTRIBUTION STATEMENT (of the abstract entered in Block 20, if different from Report)		
18. SUPPLEMENTARY NOTES APPROVED FOR PUBLIC RELEASE: IAW AFR 190-1		<p><i>Lynn E. Wolaver</i> LYNN E. WOLAVER 17 April 86 Dean for Research and Professional Development AFIT/NR, WPAFB OH 45433-6583</p>
19. KEY WORDS (Continue on reverse side if necessary and identify by block number)		
20. ABSTRACT (Continue on reverse side if necessary and identify by block number)		

DTIC FILE COPY

DTIC
ELECTE
MAY 02 1986
E

NEW NON-LINEAR FM PULSE-COMPRESSION
TECHNIQUE FOR RADAR APPLICATIONS

BY

RONALD A. BOOHER, 2LT USAF

1985

60 Pages

62

Accession For	
NTIS GRA&I	<input checked="" type="checkbox"/>
DTIC TAB	<input type="checkbox"/>
Unannounced	<input type="checkbox"/>
Justification	
By _____	
Distribution/	
Availability Codes	
Dist	Avail and/or Special
A-1	

Degree Awarded: Master of Science in Engineering

Institution: University of Central Florida

ABSTRACT

The development of pulsed type radar signals is examined, with a brief review of matched filtering. Gated RF linear and nonlinear FM pulse-compression (chirp) and matched filtering of radar signals is reviewed in depth. Emphasis is given to identifying the desirable properties of each method.

A new method of non-linear FM pulse-compression is introduced; it utilizes the Eigen Function (a form of the raised-cosine family of functions) as its modulating term. Its properties are then compared to those of the linear and nonlinear systems reviewed in the preceding sections. Design considerations for implementation on a surface acoustic wave device are presented.

MAJOR REFERENCES:

- Cook, Charles E., and Bernfield, Marvin. Radar Signals - An Introduction to Theory and Application. New York: Academic Press, 1967.
- Malocha, D.C., and Richie, S.M. "Computer Aided Design of Surface Acoustic Wave Bi-directional Transducers." Final Report to Texas Instruments, March 1984.
- Ristic, Velimir M. Principles of Acoustic Devices. New York: John Wiley and Sons, Inc., 1983.

86 5 1 060

UNIVERSITY OF CENTRAL FLORIDA
OFFICE OF GRADUATE STUDIES

THESIS APPROVAL

DATE: December 6, 1985

I HEREBY RECOMMEND THAT THE THESIS PREPARED UNDER MY SUPERVISION

BY Ronald A. Booher

ENTITLED "New Non-Linear FM Pulse-Compression
Technique for Radar Applications"

BE ACCEPTED IN PARTIAL FULFILLMENT OF THE REQUIREMENTS OF THE
DEGREE OF Master of Science in Engineering

FROM THE COLLEGE OF Engineering

Masjid Belkerdid
Masjid Belkerdid
Supervisor of Thesis

RECOMMENDATION CONCURRED IN:

Ronald L. Phillips

Parveen Wahid

Robert L. Walker

Donald C. Malocha
COMMITTEE ON FINAL EXAMINATION

Bruce E. Mathews
Coordinator of Degree Program

Louis M. Trefonas
Dean of Graduate Studies

NEW NON-LINEAR FM PULSE-COMPRESSION
TECHNIQUE FOR RADAR APPLICATIONS

BY

RONALD A. BOOHER
B.S.E., University of Central Florida, 1984

THESIS

Submitted in partial fulfillment of the requirements
for the degree of Master of Science in Engineering
in the Graduate Studies Program of the College of Engineering
University of Central Florida
Orlando, Florida

Fall Term
1985

ACKNOWLEDGEMENTS

I would like to thank my committee, especially my chairman, Dr. Belkerdid, for their support and assistance in this endeavor. I would also like to thank the members of the Solid State Devices Lab for their encouragement and assistance. A special thank you to my wife, Nancy, for her support, patience and understanding over the period of this work.

TABLE OF CONTENTS

LIST OF TABLES	v
LIST OF FIGURES	vi
Chapter	
I. DEVELOPMENT OF PULSED RADAR SIGNAL PROCESSING	1
The Theory of Matched Filter Signal Processing	1
Pulse-Compression Concepts	6
Gated RF Pulsed Radar Techniques	7
Linear FM Pulse-Compression Systems	14
Non-Linear FM Pulse-Compression Techniques	24
II. OBJECTIVE OF PROPOSED WORK	26
III. INTRODUCTION AND EVALUATION OF NEW NON-LINEAR PULSE-COMPRESSON TECHNIQUE	27
Theory and Closed Form Analysis	27
Comparison of Properties with Linear and Non-Linear FM Systems	39
Design Procedures and Considerations	45
IV. CONCLUSION AND SUMMARY	51
REFERENCES	53

LIST OF TABLES

1. Auto-Correlation Sidelobe Comparisons for Non-Linear FM with Cosine ⁿ Output Spectra	24
2. Characteristics of New Non-Linear FM and Linear FM with a Time-Bandwidth Product of 4.8	41
3. Characteristics of New Non-Linear FM and Linear FM with a Time-Bandwidth Product of 4.8 and a Cosine Window on all Signals	43

LIST OF FIGURES

1.	Block Diagram of the Receiver Matched Filter for Gated RF	8
2.	Plot of Received Signal, $s(t)$, for Gated RF Pulsed Radar .	10
3.	Gated RF Signal Spectrum (Frequency Response)	10
4.	Auto-Correlation Function for a Gated RF Pulse Matched Filter System Output	13
5.	Plot of a Sample Linear FM Transmitted Signal	16
6.	Plot of Linear FM Frequency Response (Spectrum)	19
7.	Matched Filter Impulse Response for a Linear FM System . .	19
8.	Linear FM Matched Filter Frequency Response	21
9.	Auto-Correlation Function for a Matched Filter Linear FM Pulse-Compression System	23
10.	Block Diagram of the Receiver Matched Filter for a New Non-Linear FM Pulse-Compression System	28
11.	Plot of $h_{31}(t)$ Eigen Function ($-\frac{T}{2} \leq t \leq \frac{T}{2}$)	30
12.	Portion of Eigen Function Used to Modulate the Received Signal	30
13.	Plot of New Non-Linear FM Received Signal	31
14.	Plot of New Non-Linear FM Spectrum	38
15.	New Non-Linear FM Matched Filter Impulse Response	38
16.	New Non-Linear FM Matched Filter Output Spectrum	40
17.	New Non-Linear FM Auto-Correlation	40
18.	Plot of Auto-Correlation Function for New Non-Linear FM, $\tau\Delta f = 4.8$	42

19.	Plot of Auto-Correlation Function for Linear FM, $\tau\Delta f = 4.8$	42
20.	Plot of Auto-Correlation Function for New Non-Linear FM with Cosine Window, $\tau\Delta f = 4.8$	44
21.	Plot of Auto-Correlation Function for Linear FM with Cosine Window	44
22.	Determining Electrode (Finger) Placement at Time t_m	46
23.	Sketch of Electrode (Finger) Placement for New Non-Linear FM	49
24.	Sketch Showing Finger Placement and Amplitude Weighting	50

CHAPTER I
DEVELOPMENT OF PULSED RADAR SIGNAL PROCESSING

The Theory of Matched Filter Signal Processing

The basic concept of matched filtering evolved from an effort to obtain a better theoretical understanding of the factors leading to optimum performance of radar systems. Matched filtering is the optimum linear processing for radar signals (Cook and Bernfeld 1967). It transforms the raw radar data, at the receiver input and in the presence of White Gaussian noise, into a form that yields optimum detection decisions. Some of these decisions might be target or no target or for estimating target parameters of range and velocity with minimum rms errors, and also for obtaining maximum resolution among a group of targets.

The characteristics of matched filters can be designated by either a frequency response function or a time response function, each being related to the other by a Fourier transform operation. In the frequency domain, the matched filter has a transfer function, $H(\omega)$, that is the complex conjugate of the spectrum of the signal that is to be processed.

$$H(\omega) = KS^*(\omega)e^{-j\omega T_d} \quad (1)$$

where $S(\omega)$ is the spectrum of the input (received) signal, $s(t)$, and T_d is a delay constant required to make the filter physically realizable.

The K is a normalizing factor required to yield a unity gain. K and T_d can be ignored in formulating the underlying relationships.

$$H(\omega) = S^*(\omega)$$

The corresponding time domain relationship is obtained from the inverse Fourier transform of $H(\omega)$. The result being that the impulse response of the matched filter is the time inverse of the known signal function. If $h(t)$ represents the matched filter impulse response, the relationship can be written as follows:

$$h(t) = KS(T_d - t) \quad (2)$$

Again, ignoring K and T_d , the basic relationship is:

$$h(t) = S(-t) \quad (3)$$

This matched filter relationship can be derived through optimization of several different characteristics. One method of deriving the matched filter relationship is to optimize the signal-to-noise ratio. The following is a reiteration of this development as shown by Cook and Bernfeld (1967).

The following section is devoted to showing that the matched filter is the optimum signal processing to maximize the signal-to-noise ratio. The signal-to-noise ratio (S/N) can be defined as:

$$\frac{S}{N} = \frac{\text{Peak Instantaneous Output Signal Power}}{\text{Output Noise Power}} \quad (4)$$

The objective here is to determine the properties of the linear system (filter) that maximize the S/N ratio as defined previously. By definition, the peak instantaneous output signal power is the square of the maximum signal output voltage, $g(t)$, in the absence of noise and assuming an output impedance of 1 ohm.

$$g(t) = \frac{1}{2\pi} \int_{-\infty}^{\infty} S(\omega) H(\omega) e^{j\omega t} d\omega \quad (5)$$

where $S(\omega)$ is the signal spectrum and $H(\omega)$ is the system transfer function. Let $t = T_d$ be the time when $g(t)$ is desired to be a maximum, where T_d is equal to or greater than the signal duration. Then:

$$g(T_d) = \frac{1}{2\pi} \int_{-\infty}^{\infty} S(\omega) H(\omega) e^{j\omega T_d} d\omega \quad (6)$$

The normalized noise power at the filter output is expressed as:

$$\sigma^2 = \frac{N_0}{2} \int_{-\infty}^{\infty} |H(\omega)|^2 \frac{1}{2\pi} d\omega \quad (7)$$

where N_0 is the single-sided noise power density, in watts/cycle/second, at the filter input. The S/N ratio to be maximized is:

$$\frac{S}{N} = \frac{g^2(T_d)}{\sigma^2} \quad (8)$$

The optimization will be accomplished in terms of finding the best $H(\omega)$ when all other parameters are fixed. This can be accomplished

by using Schwarz's inequality. The signal-to-noise ratio to be maximized is then:

$$\frac{S}{N} = \frac{\left| \frac{1}{2\pi} \int_{-\infty}^{\infty} S(\omega) H(\omega) e^{j\omega T_d} d\omega \right|^2}{\frac{N_0}{4\pi} \int_{-\infty}^{\infty} |H(\omega)|^2 d\omega} \quad (9)$$

where Schwarz's inequality is given by: (10)

$$\left| \frac{1}{2\pi} \int_{-\infty}^{\infty} X_1(\omega) X_2(\omega) d\omega \right|^2 \leq \frac{1}{2\pi} \int_{-\infty}^{\infty} |X_1(\omega)|^2 d\omega \frac{1}{2\pi} \int_{-\infty}^{\infty} |X_2(\omega)|^2 d\omega$$

where $X_1(\omega)$ and $X_2(\omega)$ are two arbitrary functions.

Equation (10) can be rewritten as:

$$\frac{\left| \int_{-\infty}^{\infty} X_1(\omega) X_2(\omega) d\omega \right|^2}{\int_{-\infty}^{\infty} |X_1(\omega)|^2 d\omega} \leq \int_{-\infty}^{\infty} |X_2(\omega)|^2 d\omega \quad (11)$$

The right side of equation (11) is maximized when (Gradshteyn and Ryzhik 1980):

$$X_1(\omega) = k_1 X_2^*(\omega) \quad (12)$$

If:

$$X_1(\omega) = \frac{N_0}{2} |H(\omega)|^2 \quad (13)$$

and:

$$X_2(\omega) = S(\omega) H(\omega) e^{j\omega T_d} \quad (14)$$

Then, according to Schwarz's inequality, equation (9), the signal-to-noise ratio is maximized when:

$$\frac{N_0}{2} |H(\omega)|^2 = k_1 S^*(\omega) H^*(\omega) e^{-j\omega T_d} \quad (15)$$

which simplifies to:

$$\frac{N_0}{2} |H(\omega)| |H(\omega)|^* = k_1 S^*(\omega) H^*(\omega) e^{-j\omega T_d} \quad (16)$$

Solving for $H(\omega)$ yields:

$$H(\omega) = \frac{2k_1}{N_0} S^*(\omega) e^{-j\omega T_d} \quad (17)$$

But since k_1 and N_0 are constants, equation (17) can be rewritten as:

$$H(\omega) = k S^*(\omega) e^{-j\omega T_d} \quad (18)$$

where:

$$k = \frac{2k_1}{N_0}$$

Therefore, applying the complex conjugate and time delay properties of the Fourier transform, the impulse response of the matched filter is given by:

$$h(t) = \mathcal{F}^{-1} \{H(\omega)\} = K S(T_d - t) \quad (19)$$

Pulse-Compression Concepts

The concept of pulse-compression was conceived out of a need to improve on the performance of pulsed radar systems. Near the end of World War II, the need for radically improved radar performance became apparent (Cook 1960). It also became obvious that Gated RF could not provide this improved performance due to power limitations of the transmitters. These limitations existed in two areas. The peak power available in the transmitter tubes was limited, and secondly, many of the transmitter components could not have operated under any higher power conditions. One possible solution to the problem would have been to increase the average power capabilities of the transmitter tubes by going to wider pulse widths. This would provide greater range capabilities, but the conflicting requirement of improved resolution for ground mapping and separation of aircraft targets in massed formations would be undermined. Therefore, this most obvious method of improvement was not acceptable.

The proposed solution to the problem of trying to improve radar performance was conceived by several individuals serving on both sides

during the war (Cook and Bernfeld 1967). The solution basically provided that a wide pulse be transmitted, during which the carrier frequency would be linearly swept. This was seen to yield a correlation between time and frequency that could be exploited in the receiver. This would be accomplished by using a filter having a linear time delay versus frequency characteristics such that it would apparently delay one end of the received wide pulse by a greater amount than the other, thus causing the signal to compress in time and increase in peak amplitude. Thus was born the concept of pulse-compression. Actual implementation did not occur until the early 1950s when the high power Klystron was developed.

Gated RF Pulsed Radar Techniques

The concept of the gated RF pulse was dominant in radar applications until the post-World War II period (Barton 1976). The basic concept is to transmit a short burst of high energy, uniform amplitude and constant frequency RF (radio frequency) signal and wait for a return signal reflected off a target. A matched filter is used in the receiver to process the return signal and yield an output signal that contains valuable information concerning target range and velocity. A block diagram of the receiver matched filter is shown in Figure 1.

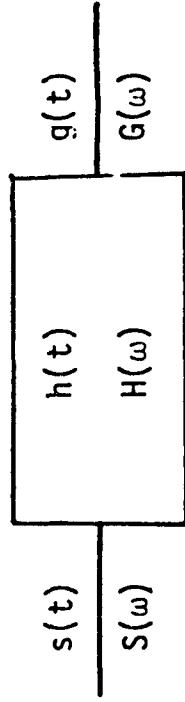


Figure 1. Block Diagram of the Receiver Matched Filter for Gated RF.

where:

$s(t)$ = the ideal return signal (transmitted signal)

$S(\omega)$ = the received signal spectrum

$h(t)$ = the matched filter impulse response

$H(\omega)$ = the matched filter spectrum

$g(t)$ = the auto-correlation output signal

$G(\omega)$ = the spectrum of the output signal

The output auto-correlation function, $g(t)$, for gated RF can be obtained from a very simple and straightforward closed form analysis. The received signal, $s(t)$, shown in Figure 2, can be expressed:

$$s(t) = \cos \omega_0 t \quad 0 \leq t \leq T$$

This can be written in terms of a rect function as:

$$s(t) = \cos \omega_0 t \cdot \text{rect} \left(\frac{t - \frac{T}{2}}{T} \right)$$

Now, applying simple Fourier transform pairs yields an expression for the spectrum, $S(f)$, as follows:

$$S(f) = \left[\frac{1}{2} \delta(f - f_0) + \frac{1}{2} \delta(f + f_0) \right] * [T \text{SINC } fT]$$

where * denotes the convolution in the frequency domain. Completing the convolution will yield frequency shifted SINC functions as follows:

$$S(f) = \frac{T}{2} \text{SINC} (f - f_0)T + \frac{T}{2} \text{SINC} (f + f_0)T \quad (20)$$

Here, it will be assumed that f_0 is a great enough value such that the negative frequency portion has negligible effect in the positive frequency range. Figure 3 shows a plot of the positive spectrum. The spectrum is the familiar $\frac{\text{SINX}}{X}$ shape with -13 dB side lobes. The center frequency

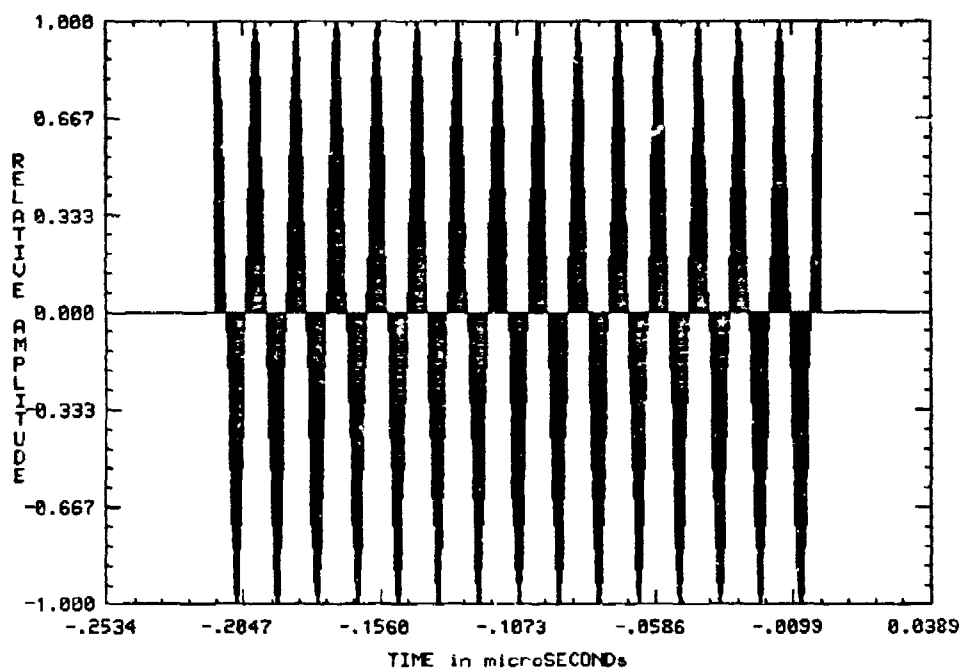


Figure 2. Plot of Received Signal, $s(t)$, for Gated RF Pulsed Radar.

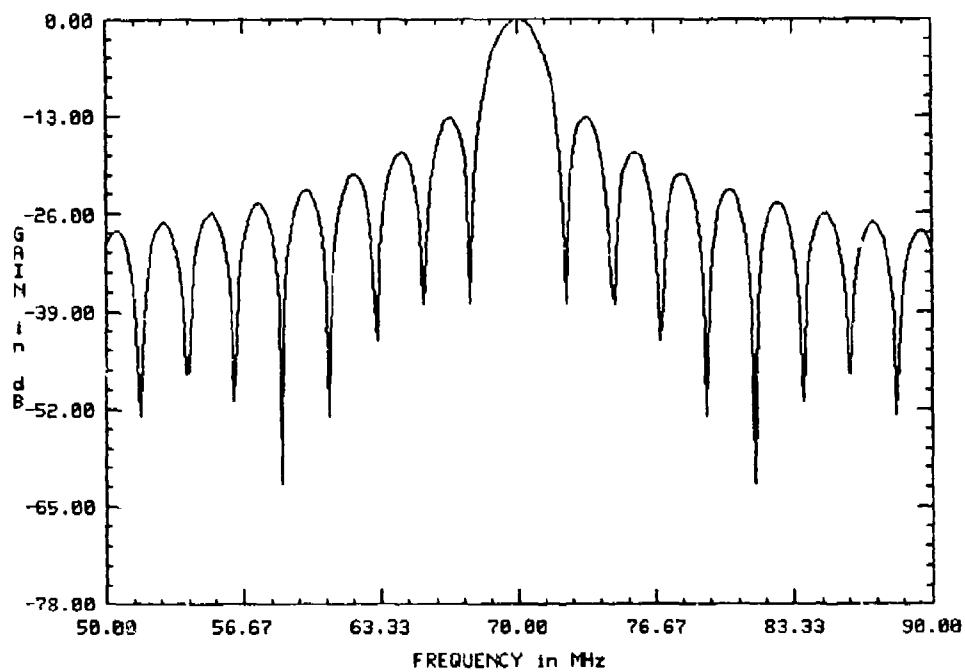


Figure 3. Gated RF Signal Spectrum (Frequency Response).

(carrier), f_0 , is 70 MHz. This same carrier frequency will be used throughout this paper.

Since all systems considered in this paper are matched filter systems, the matched filter case will be investigated here. The matched filter impulse response, $h(t)$, can be written as:

$$\begin{aligned} h(t) &= s(T - t) \\ &= \cos [\omega_0 (T - t)] \cdot \text{rect} \left(\frac{T - t - \frac{T}{2}}{T} \right) \end{aligned}$$

Now noting that $\text{rect} \left(\frac{-(t - \frac{T}{2})}{T} \right)$ can be written as $\text{rect} \left(\frac{t - \frac{T}{2}}{T} \right)$ and

letting $\omega_0 = \frac{2\pi K}{T}$, where $K = \text{integer}$. The impulse response, $h(t)$, can be rewritten as:

$$\begin{aligned} h(t) &= \cos [\omega_0 T - \omega_0 t] \cdot \text{rect} \left(\frac{t - \frac{T}{2}}{T} \right) \\ &= \cos [2\pi K - \omega_0 t] \cdot \text{rect} \left(\frac{t - \frac{T}{2}}{T} \right) \end{aligned}$$

Now with simple trigonometric identities, $h(t)$ becomes:

$$h(t) = [\cos(2\pi K) \cos(\omega_0 t) + \sin(2\pi K) \sin(\omega_0 t)] \cdot \text{rect} \left(\frac{t - \frac{T}{2}}{T} \right)$$

Since $\cos(2\pi K) = 1$ and $\sin(2\pi K) = 0$, this becomes:

$$h(t) = \cos(\omega_0 t) \cdot \text{rect} \left(\frac{t - \frac{T}{2}}{T} \right)$$

This is identical to the received signal, $s(t)$. Therefore, the matched filter spectrum, $H(\omega)$, will be identical to $S(\omega)$. The reader is referred to figures 2 and 3 for plots of these functions.

The desired output from the matched filter, the auto-correlation function, can be obtained analytically by doing the actual convolution where:

$$\begin{aligned} g(t) &= s(t) * h(t) \\ &= \int_{-\infty}^{\infty} s(\tau) h(t - \tau) d\tau \end{aligned}$$

or by finding $G(\omega)$ and taking the inverse Fourier transform:

$$G(f) = [S(f)]^2$$

which, considering only positive frequencies, can be written as:

$$G(f) = \frac{T^2}{4} \text{SINC}^2 [(f - f_c)T]$$

Now using a very common Fourier transform pair, $g(t)$ can be written directly as:

$$g(t) = \begin{cases} \frac{t}{2} \cos \omega_0 t & 0 \leq t \leq T \\ (T - \frac{t}{2}) \cos \omega_0 t & T \leq t < 2T \\ 0 & \text{otherwise} \end{cases}$$

Figure 4 is a plot of the magnitude of $g(t)$ obtained from the Surface Acoustic Wave Computer-Aided Design program (SAWCAD) by squaring the signal spectrum, $S(f)$ (see Figure 3) and then taking the inverse FFT (Fast Fourier Transform). Due to the FFT processing, only the positive portion of the signal is plotted.

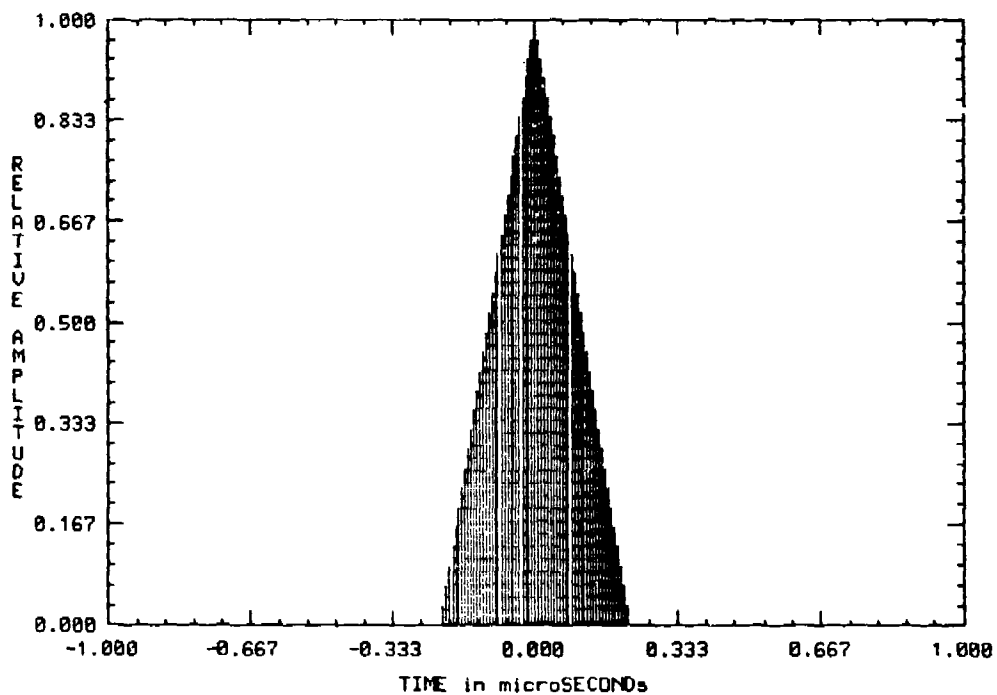


Figure 4. Auto-Correlation Function for a Gated RF Pulse Matched Filter System Output.

Linear FM Pulse-Compression Systems

Initial implementation of pulse-compression was in the form of linear FM (Klauder et al. 1960). It is currently the most widely used type of pulse-compression waveforms. Linear FM pulse-compression is easy to implement and for a majority of radar applications it has the best overall properties. In general, linear FM waveforms provide improvement over Gated RF by satisfying five basic requirements.

These requirements are (Ramp and Wingrove 1961):

1. A product of bandwidth and duration greater than unity (for good resolution of both range and velocity)
2. A rectangular amplitude spectrum (for best range resolution)
3. A rectangular envelope (for best velocity resolution)
4. Phase dispersion (that is, a non-linear phase spectrum to permit pulse-compression)
5. Phase matching can be accomplished using a single filter

Here, linear FM pulse-compression will be examined in the same type of matched filter system as the Gated RF was. The transmitted waveform for the linear FM pulse-compression signal is written:

$$s(t) = \cos[\omega_0 t + \frac{\mu}{2} t^2] \quad -\frac{T}{2} \leq t \leq \frac{T}{2} \quad (21)$$

$$= 0 \quad \text{elsewhere}$$

where:

- ω_0 = carrier frequency (radians/sec)
- μ = rate of frequency sweep ($\Delta\omega/T$)
- $\Delta\omega$ = swept spectrum bandwidth (μT)
- T = uncompressed pulse width

Figure 5 is a plot of a sample linear FM signal.

The spectrum of the linear FM signal can be expressed by the following:

$$\begin{aligned}
 S(\omega) &= \int_{-\frac{T}{2}}^{\frac{T}{2}} \cos\left[\omega_0 t + \frac{\mu t^2}{2}\right] e^{-j\omega t} dt \\
 &= \frac{1}{2} \int_{-\frac{T}{2}}^{\frac{T}{2}} e^{j[(\omega_0 - \omega)t + \frac{\mu t^2}{2}]} dt \\
 &\quad + \int_{-\frac{T}{2}}^{\frac{T}{2}} e^{-j[(\omega_0 + \omega)t + \frac{\mu t^2}{2}]} dt
 \end{aligned} \tag{22}$$

where the first integral defines the positive frequency spectrum and the second integral defines the negative frequency spectrum. Since the negative frequency spectrum has a negligible contribution at positive frequencies, it will be ignored here. By completing the square of the bracketed term in equation (22), the spectrum becomes:

$$S(\omega) = \frac{1}{2} e^{-j\left(\frac{\omega - \omega_0}{2\mu}\right)^2} \int_{-\frac{T}{2}}^{\frac{T}{2}} e^{j\left[\frac{\mu}{2}\left(t + \frac{\omega - \omega_0}{\mu}\right)^2\right]} dt \tag{23}$$

Using the change of variable:

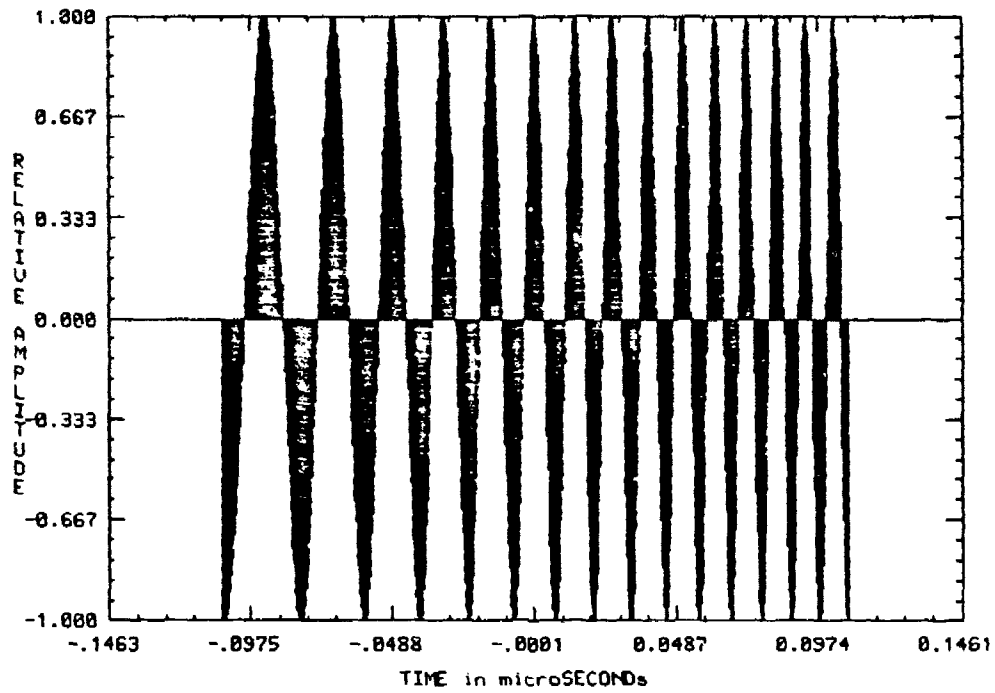


Figure 5. Plot of a Sample Linear FM Transmitted Signal.

$$\sqrt{\mu} \left(t - \frac{\omega - \omega_0}{\mu} \right) = \sqrt{\pi} x$$

and

$$dt = \sqrt{\frac{\pi}{\mu}} dx$$

The spectrum can now be written:

$$S(\omega) = \frac{1}{2} \sqrt{\frac{\pi}{\mu}} e^{-j \left(\frac{\omega - \omega_0}{2\mu} \right)^2} \int_{-x_1}^{x_2} e^{j \frac{\pi x^2}{2}} dx \quad (24)$$

where:

$$x_1 = \frac{\frac{\mu T}{2} + (\omega - \omega_0)}{\sqrt{\pi \mu}}$$

and

$$x_2 = \frac{\frac{\mu T}{2} - (\omega - \omega_0)}{\sqrt{\pi \mu}}$$

The spectrum can now be expressed in terms of the Fresnel integrals as:

$$S(\omega) = \frac{1}{2} \sqrt{\frac{\pi}{\mu}} e^{-j \left(\frac{(\omega - \omega_0)^2}{2\mu} \right)} [C(x_1) + jS(x_1) + C(x_2) + jS(x_2)] \quad (25)$$

The above expression for the linear FM spectrum can be broken down into three components:

Amplitude Term:

$$|S(\omega)| = \frac{1}{2} \sqrt{\frac{\pi}{\mu}} \{ [C(x_1) + C(x_2)]^2 + [S(x_1) + S(x_2)]^2 \}^{\frac{1}{2}}$$

Square Law Phase Term:

$$\phi_1 = \frac{(\omega_0 - \omega)^2}{2\mu}$$

and:

Residual Phase Term:

$$\phi_2 = - \tan^{-1} \left[\frac{S(X_1) + S(X_2)}{C(X_1) + C(X_2)} \right]$$

where:

$$C(X) = \int_0^X \cos \frac{\pi y^2}{2} dy$$

and

$$S(X) = \int_0^X \sin \frac{\pi y^2}{2} dy$$

are the well-known Fresnel integrals.

An illustrated plot of the received signal spectrum, $S(\omega)$, is shown in Figure 6. The actual plotting was accomplished using the FFT and graphics capabilities of SAWCAD.

Now, using matched filter principles, the impulse response of the matched filter can be written directly as the time inverse of the transmitted signal.

$$h(t) = \sqrt{\frac{2\mu}{\pi}} \cos\left[\omega_0 t - \frac{\mu t^2}{2}\right] \quad -\frac{T}{2} \leq t \leq \frac{T}{2} \quad (26)$$

= 0

elsewhere

where $\sqrt{2\mu/\pi}$ is the normalizing factor required to give the filter unity gain. An illustration of the matched filter impulse response, $h(t)$, is shown in Figure 7.

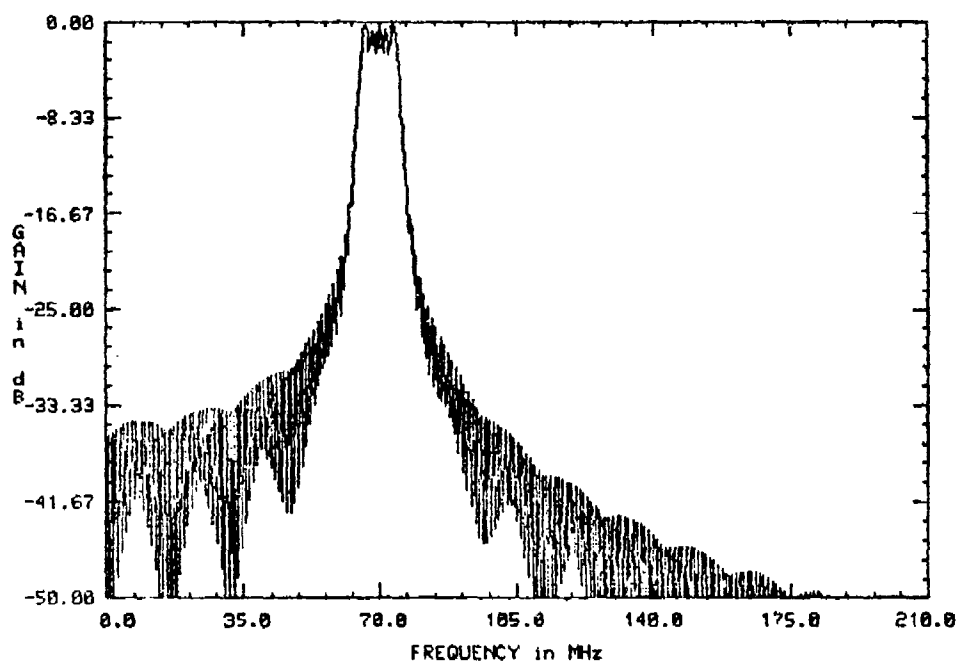


Figure 6. Plot of Linear FM Frequency Response (Spectrum).

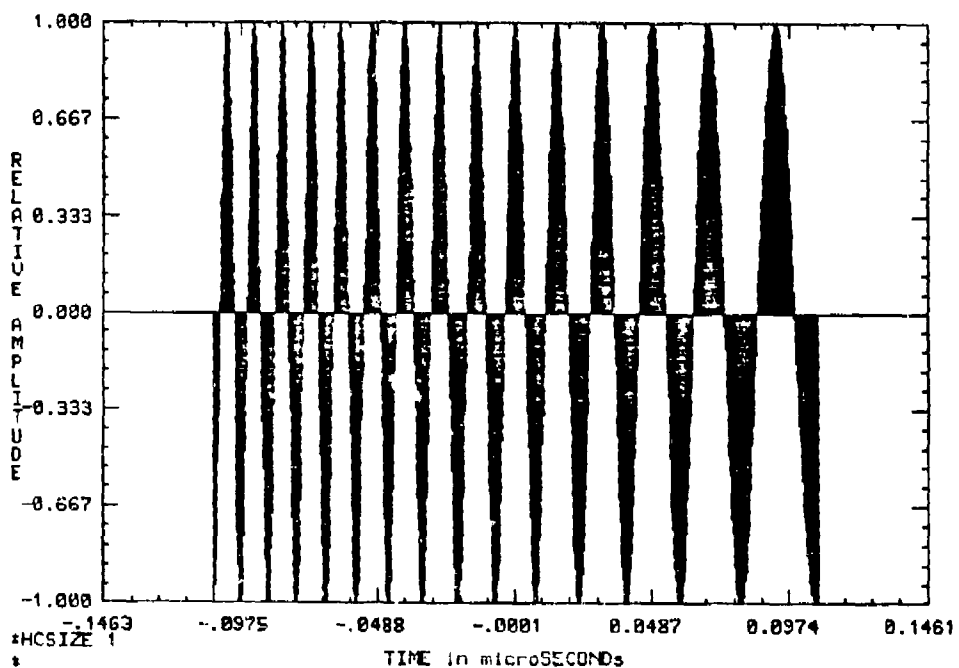


Figure 7. Matched Filter Impulse Response for a Linear FM System.

To obtain the matched filter frequency spectrum, the matched filter relationship, $H(\omega) = S^*(\omega)$, is used to write $H(\omega)$ as:

$$\begin{aligned} H(\omega) = S^*(\omega) &= |S(\omega)| e^{-j(\phi_1 + \phi_2)} \\ &= \frac{1}{2} \sqrt{\frac{\pi}{\mu}} \{ [C(X_1) + C(X_2)]^2 + [S(X_1) + S(X_2)]^2 \} e^{-j\left(\frac{(\omega - \omega_0)^2}{2\mu}\right)} \end{aligned} \quad (27)$$

where ϕ_1 is the square law phase term:

$$\phi_1 = \frac{(\omega_0 - \omega)^2}{2\mu} \quad (28)$$

and ϕ_2 is the residual phase term:

$$\phi_2 = -\tan^{-1} \left[\frac{S(X_1) + S(X_2)}{C(X_1) + C(X_2)} \right] \quad (29)$$

The residual phase term can be neglected here because it can be approximated by a constant phase term over the spectrum bandwidth, Δf . Figure 8 is an illustration of the matched filter spectrum, $H(\omega)$.

The output of the matched filter is the auto-correlation function of the input signal, $s(t)$. This function can be obtained by convolving the input signal, $s(t)$, with the matched filter impulse response, $h(t)$, yielding:

$$g(t) = \int_{-\infty}^{\infty} S(\tau) h(T - \tau) d\tau \quad (30)$$

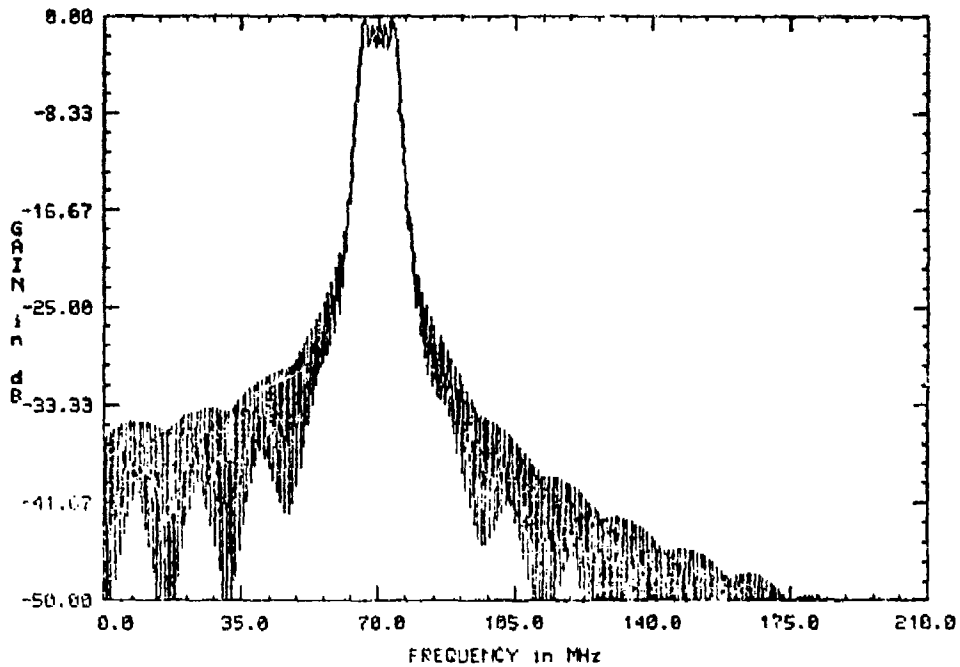


Figure 8. Linear FM Matched Filter Frequency Response.

Another method is to multiply the input signal spectrum by the matched filter spectrum and then take the inverse Fourier transform, yielding:

$$g(t) = \mathcal{F}^{-1} \{G(\omega)\} = \mathcal{F}^{-1} \{S(\omega) \cdot H(\omega)\} \quad (31)$$

Using this second method, $g(t)$ can be derived in the following manner:

$$g(t) = \mathcal{F}^{-1} \{S(\omega) \cdot H(\omega)\} = \mathcal{F}^{-1} \{G(\omega)\} \quad (32)$$

where:

$$\begin{aligned} G(\omega) &= S(\omega) \cdot H(\omega) = S(\omega) \cdot S^*(\omega) \\ &= |S(\omega)|^2 \end{aligned} \quad (33)$$

Substituting for $S(\omega)$ yields:

$$G(\omega) = \left| \frac{1}{2} \sqrt{\frac{\pi}{\mu}} \{ [C(X_1) + C(X_2)]^2 + [S(X_1) + S(X_2)]^2 \}^{1/2} \right|^2 \quad (34)$$

$$= \frac{1}{4} \frac{\pi}{\mu} \{ [C(X_1) + C(X_2)]^2 + [S(X_1) + S(X_2)]^2 \} \quad (35)$$

Taking the inverse Fourier transform yields the following result:

$$g(t) = \sqrt{\frac{2\mu}{\pi}} \frac{\sin \left[\frac{\mu t}{2} (T - |t|) \right]}{\mu T} \cos(\omega_0 t) \quad -T \leq t \leq T \quad (36)$$

This equation now represents the usable output from the matched filter and with further receiver processing can provide information concerning range, velocity and dimension about a target. By definition, $\Delta f = \mu T / 2\pi$ and $1/T\Delta f$, where the latter is the amount the output pulse width has been reduced. The factor, $T\Delta f$, defines a pulse width ratio of the input and output functions known as the compression-ratio. This same factor represents the amount the peak power level has increased over the Gated RF case. Figure 9 is a plot of the auto-correlation function for a sample linear FM signal.

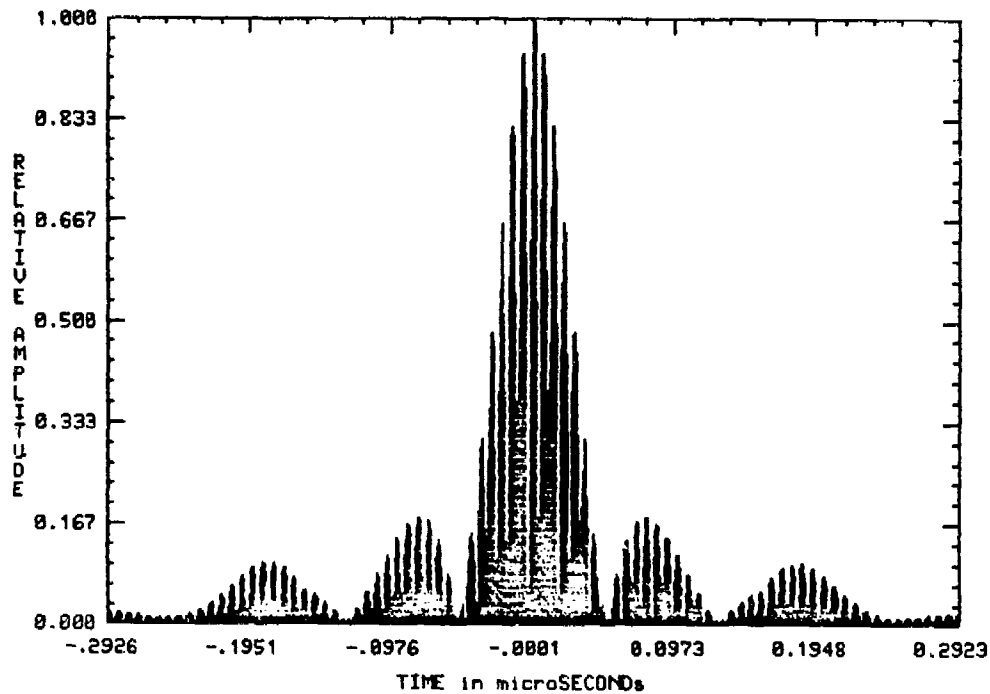


Figure 9. Auto-Correlation Function for a Matched Filter Linear FM Pulse-Compression System.

Linear FM pulse compression has provided the necessary improvement, in range, velocity and resolution, over Gated RF. But, linear FM still has its shortcomings. One such weakness is that the auto-correlation function has fairly high sidelobes; these sidelobes increase as the compression ratio is increased. Several filtering techniques have been employed to reduce these sidelobes. One method used to suppress these sidelobes is to deliberately mismatch the amplitude response of the matched filter (Bernfeld et al. 1965). This has the effect of lowering sidelobe levels, but introduces a 1-2 dB mismatch loss.

Non-Linear FM Pulse-Compression Techniques

In an effort to overcome the mismatch loss, but still achieve low auto-correlation sidelobe levels, non-linear FM has been investigated. Non-linear FM functions with odd symmetry have been investigated (Bernfeld et al. 1965), which yield low sidelobe levels while avoiding the mismatch loss. One such class of functions yields spectra at the mismatch filter output given by:

$$|G(\omega)| = \cos^n \left[\frac{\pi(\omega_0 - \omega)}{\Delta\omega} \right] \quad \text{for} \quad |\omega_0 - \omega| \leq \frac{\Delta\omega}{2}$$

The matched filter auto-correlation waveform of these signals is:

$$g(t) = \frac{1}{2\pi} \int_{\omega_0 - \frac{\Delta\omega}{2}}^{\omega_0 + \frac{\Delta\omega}{2}} \cos^n \left[\frac{\pi(\omega_0 - \omega)}{\Delta\omega} \right] e^{j(\omega_0 - \omega) t_d} (\omega_0 - \omega)$$

The authors' results are given in Table 1 (Cook et al. 19).

TABLE 1
AUTO-CORRELATION SIDELOBE COMPARISONS FOR NON-LINEAR
FM WITH COSINEⁿ OUTPUT SPECTRA

n	$\frac{\Delta\omega_n}{\Delta\omega_1}$	SIDELOBE
1	1.00	-23 dB
2	1.21	-32 dB
3	1.40	-40 dB

It should be noted that non-linear FM is only suitable for applications in which the expected range of Doppler frequency shifts is quite small.

Another example of using a non-linear FM waveform to achieve low time sidelobes has been presented in which the author was able to achieve -27 dB sidelobes in a system with a time-bandwidth product of 22 and a 0.1 dB mismatch loss (Millett 1970). This was achieved by choosing a particular weighting function of the expanded pulse spectrum. In particular:

$$|F(\omega)| = \sqrt{K + (1 - K) \cos^2 \frac{\omega}{2\Delta}}$$

where K is the amplitude of the output spectrum and Δ is the signal bandwidth. Then, by employing a receiver with an amplitude response that has the same variation with frequency and a dispersion of the opposite sense as that in the received signal, the system is a matched filter system with "cosine squared on a pedestal" weighting. Each dispersive filter in this case was synthesized as a cascade of bridged-tee networks.

Both of these techniques proved to be usable; however, the design methods are complicated and iterative. In the next section, a new non-linear FM pulse-compression waveform is investigated for design on a surface acoustic wave device.

CHAPTER II

OBJECTIVE OF PROPOSED WORK

The main objective of this thesis is to introduce, analyze and evaluate a new non-linear FM pulse-compression technique to be implemented on a surface acoustic wave (SAW) device. Although the implementation has not actually been accomplished, it is intended that it be done using a computer-aided design program, SAWCAD, developed at the University of Central Florida. Design procedures and considerations will be discussed (Malocha and Richie 1984).

CHAPTER III
INTRODUCTION AND EVALUATION OF NEW NON-LINEAR
PULSE-COMPRESSION TECHNIQUE

Theory and Closed Form Analysis

The principle benefit of using a non-linear modulating term is the reduction in auto-correlation sidelobe level and a like gain in mainlobe signal strength in a matched filter pulse-compression system. It has been shown that for many applications in which the range of Doppler shifts is quite small (stationary target), the signal auto-correlation waveform is a major consideration (Bernfeld et al. 1965). The desired auto-correlation waveform should exhibit very low sidelobes in order to reduce the masking effect of large signals on small signals not at the same range. To obtain low sidelobes with linear FM would require using a frequency weighting mismatch filter after the matched filter. This, in turn, leads to a reduction in signal-to-noise ratio relative to the ideal matched filter case. The use of a non-linear FM function as a means of obtaining matched filter waveforms with low range sidelobes, while avoiding mismatch loss, has been investigated (Cook et al. 1965).

In this section, a non-linear FM function is investigated for its potential as a low sidelobe level matched filter pulse-compression system. This system will again be considered in the general receiver configuration, as shown in Figure 10.

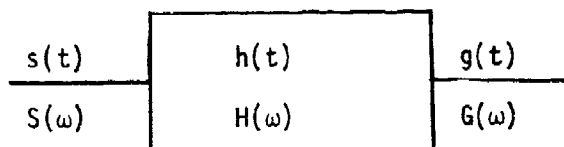


Figure 10. Block Diagram of the Receiver Matched Filter for a New Non-Linear FM Pulse-Compression System.

where:

$s(t)$ = the ideal received signal (the transmitted signal)

$S(\omega)$ = the spectrum of the received signal

$h(t)$ = the matched filter impulse response

$H(\omega)$ = the matched filter spectrum

$g(t)$ = the auto-correlation function

$G(\omega)$ = the output spectrum

Here, the non-linear FM waveform, $s(t)$, is obtained by using a form of the class of the raised-cosine family of functions known as the Eigen function. In particular, the $h_{31}(t)$ Eigen function has been utilized, where:

$$h_{31}(t) = .43 + .5 \cos\left(\frac{2\pi t}{\tau}\right) + .07 \cos\left(\frac{4\pi t}{\tau}\right)$$

This function is shown in Figure 11, plotted from $-\frac{T}{2}$ to $\frac{T}{2}$. Due to the symmetry about zero, only the portion from $-\frac{T}{2}$ to 0 is used to create the up-chirped (expanded pulse) received signal, $s(t)$. This portion of the Eigen function is shown in Figure 12.

In order to obtain a modulated frequency deviation, Δf , that is proportional to the Eigen function, it is necessary to use the integral of $h_{31}(t)$ as the phase term in $s(t)$. The non linear FM waveform is then written as:

$$s(t) = \cos\{\omega_0 t + D_f [.43t + \frac{.5T}{2\pi} \sin(\frac{2\pi t}{T}) + \frac{.07T}{4\pi} \sin(\frac{4\pi t}{T})]\}$$

$$\text{for } -\frac{T}{2} \leq t \leq \frac{T}{2} \quad \text{where } T = 2\tau$$

Now, utilizing only that portion of the signal from $-\frac{T}{2}$ to zero and maintaining a τ pulse width, $s(t)$ becomes:

$$s(t) = \cos\{\omega_0 t + D_f [.43t + \frac{.5T}{2\pi} \sin(\frac{2\pi t}{T}) + \frac{.07T}{4\pi} \sin(\frac{4\pi t}{T})]\}$$

$$\cdot \text{rect} \left[\frac{t + T/4}{T/2} \right]$$

A plot of $s(t)$, with a cosine window function applied to it, is shown in Figure 13.

One advantage this new non-linear FM has over previously examined non-linear FM signals is that its spectrum can be derived from a closed-form analysis. The following is a complete derivation of this spectrum.

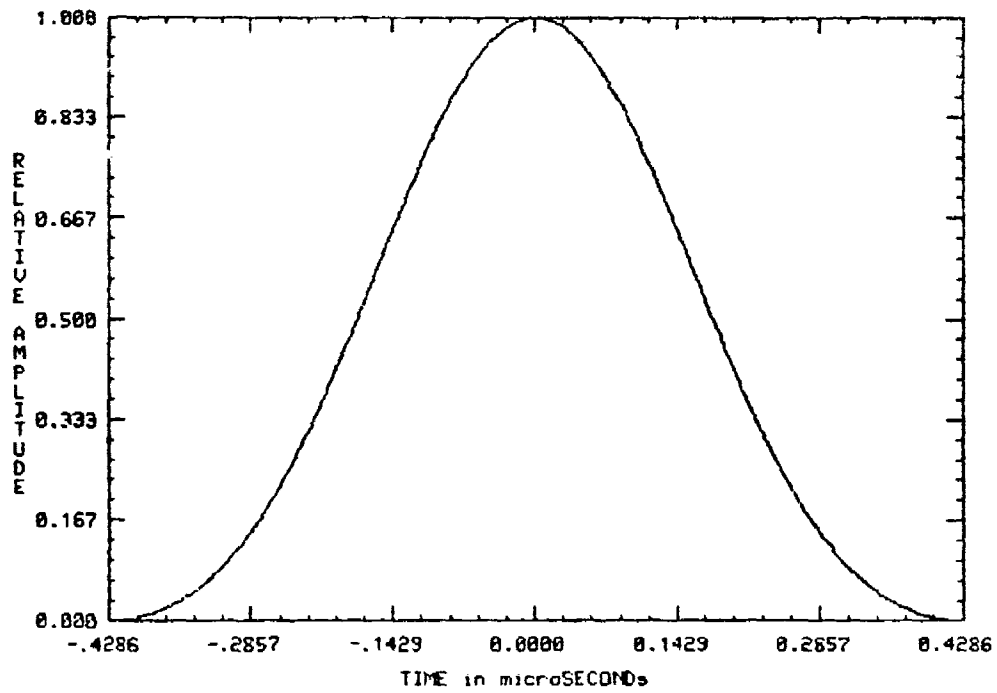


Figure 11. Plot of $h_{31}(t)$ Eigen Function ($-\frac{T}{2} \leq t \leq \frac{T}{2}$).

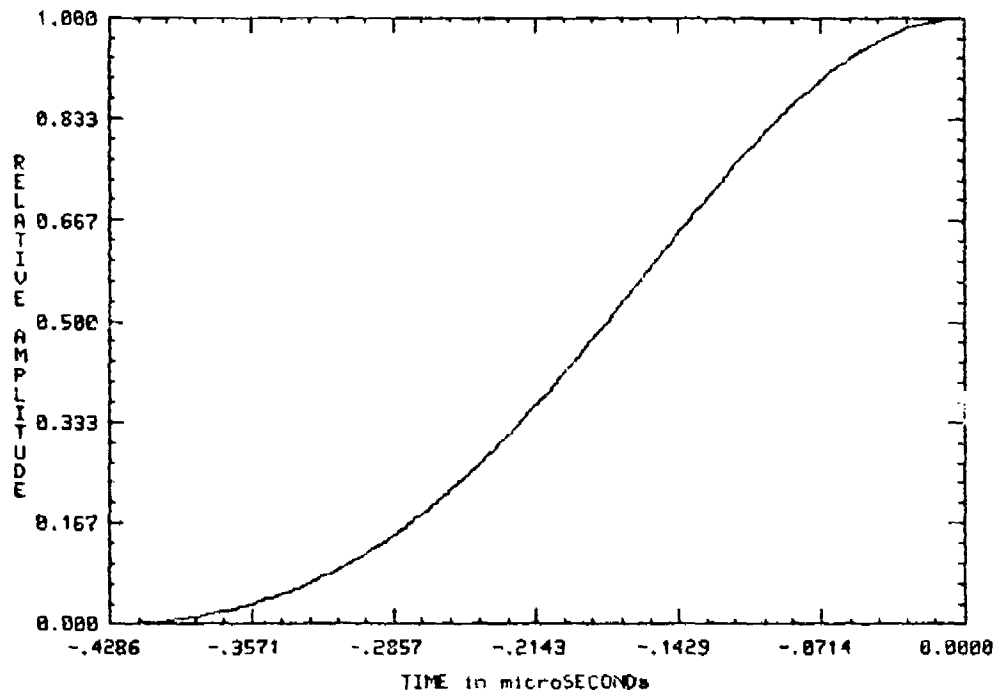


Figure 12. Portion of Eigen Function Used to Modulate the Received Signal.

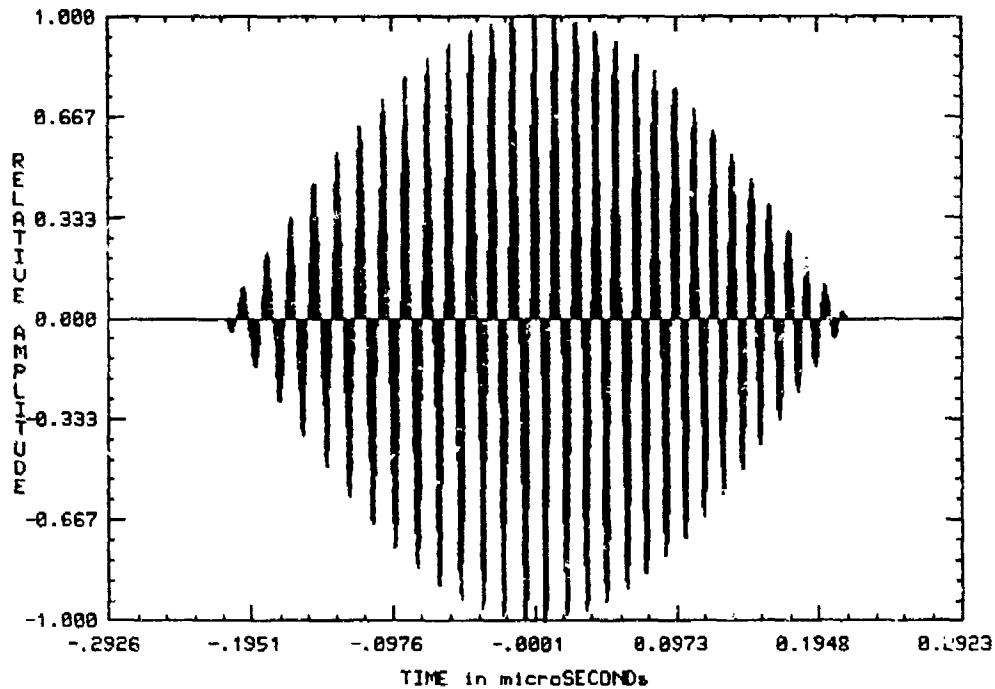


Figure 13. Plot of New Non-Linear FM Received Signal.

First, the received signal, $s(t)$, with the integral of the $h_{31}(t)$ Eigen as its phase term and a cosine window function included can be written as:

$$s(t) = \cos\left\{\omega_0 t + .43 D_f t + \frac{.5T D_f}{2\pi} \sin\left(\frac{2\pi t}{T}\right) + \frac{.07T D_f}{4\pi} \sin\left(\frac{4\pi t}{T}\right)\right\} \\ \cdot \cos\left(\frac{2\pi (t + T/4)}{T}\right) \cdot \text{rect}\left(\frac{t + T/4}{T/2}\right)$$

by making the following definitions:

$$\beta_1 = \frac{0.5T D_f}{2}$$

and

$$\beta_2 = \frac{0.07T D_f}{4\pi}$$

also:

$$m_1 = \frac{2\pi}{T}$$

and

$$m_2 = \frac{4\pi}{T}$$

$s(t)$ can now be rewritten as:

$$s(t) = \cos\{\omega_0 t + .43D_f t + \beta_1 \sin(\omega_{m1} t) + \beta_2 \sin(\omega_{m2} t)\} \\ \cdot \cos\left(\frac{2\pi(t + T/4)}{T}\right) \cdot \text{rect}\left(\frac{t + T/4}{T/2}\right)$$

Next, utilizing Euler's theorem, $e^{\pm j\omega t} = \cos \omega t \pm j \sin \omega t$, $s(t)$ can again be rewritten as:

$$s(t) = \text{Re}\{e^{j\omega_0 t} e^{j0.43D_f t} e^{j\beta_1 \sin(\omega_{m1} t)} e^{j\beta_2 \sin(\omega_{m2} t)}\} \cdot \cos\left(\frac{2\pi(t+T/4)}{T}\right) \\ \cdot \text{rect}\left(\frac{t + T/4}{T/2}\right)$$

Expanding the last two exponentials in a Fourier series yields:

$$e^{j\beta_1 \sin(\omega_{m1}t)} = \sum_{n=-\infty}^{\infty} F_n e^{jn\omega_{m1}t}$$

and

$$e^{j\beta_2 \sin(\omega_{m2}t)} = \sum_{K=-\infty}^{\infty} F_K e^{jK\omega_{m2}t}$$

where the coefficients, F_n and F_K , are represented by:

$$F_n = \frac{1}{T} \int_{-\frac{T}{2}}^{\frac{T}{2}} e^{j\beta_1 \cos(\omega_{m1}t)} e^{-jn(\omega_{m1}t)} dt$$

and

$$F_K = \frac{1}{T} \int_{-\frac{T}{2}}^{\frac{T}{2}} e^{j\beta_2 \cos(\omega_{m2}t)} e^{-jK(\omega_{m2}t)} dt$$

Next, by defining an α_1 and α_2 as follows:

$$\alpha_1 = \omega_{m1}t = \frac{2\pi t}{T}$$

and

$$\alpha_2 = \omega_{m2} t = \frac{2\pi t}{T}$$

The equations for F_n and F_K can be rewritten as:

$$F_n = \frac{1}{2\pi} \int_{-\pi}^{\pi} e^{j(\beta_1 \cos \alpha_1 - Z\alpha_1)} d\alpha_1$$

and

$$F_K = \frac{1}{2\pi} \int_{-\pi}^{\pi} e^{j(\beta_2 \cos \alpha_2 - Z\alpha_2)} d\alpha_2$$

F_n and F_K are now in the form of the easily recognizable Bessel function of the first kind, commonly written as:

$$F_n = J_n(\beta_1)$$

and

$$F_K = K_J(\beta_2)$$

Values for the Bessel function exist in tabulated form (Watson 1966) or can be obtained numerically (by computer) by evaluating the integral (Gradshteyn and Ryzhik 1980).

$$J_n(\beta) = \frac{1}{\pi} \int_0^{\pi} \cos(\beta \theta - Z \sin \theta) d\theta \quad [n - \text{a natural number}]$$

The received signal, $s(t)$, can now be expressed in terms of the Bessel functions as:

$$s(t) = \operatorname{Re} \left\{ e^{j\omega_0 t} e^{j0.48D_f t} \sum_{n=-\infty}^{\infty} J_n(\beta_1) e^{jn\omega_{m1} t} \sum_{K=-\infty}^{\infty} J_K(\beta_2) e^{jK\omega_{m2} t} \right\} \\ \cdot \cos\left(\frac{2\pi(t + T/4)}{T}\right) \cdot \operatorname{rect}\left(\frac{t + T/4}{T/2}\right)$$

Now, again using Euler's theorem, the real part of $s(t)$ can be written as a cosine such that:

$$s(t) = \sum_{n=-\infty}^{\infty} \sum_{K=-\infty}^{\infty} J_n(\beta_1) J_K(\beta_2) \cos[(\omega_0 t + 0.43D_f + n\omega_{m1} + K\omega_{m2})t] \\ \cdot \cos\left(\frac{2\pi(t + T/4)}{T/2}\right) \cdot \operatorname{rect}\left(\frac{t + T/4}{T/2}\right)$$

Since the Bessel functions are just constants, the application of some very simple Fourier transform rules will yield an expression for the spectrum, $s(f)$.

$$s(f) = \sum_{n=-\infty}^{\infty} \sum_{K=-\infty}^{\infty} J_n(\beta_1) J_K(\beta_2) \{ \delta[f - (f_0 + 0.43D_f + nf_{m1} + Kf_{m2})] \\ + \delta[f + (f_0 + 0.43D_f + nf_{m1} + Kf_{m2})] \} * \left[\delta\left(f - \frac{1}{2T}\right) e^{+j\frac{\pi}{2}} + \delta\left(f + \frac{1}{2T}\right) \right]$$

$$e^{-j\frac{\pi}{2}} \left] e * \left[\frac{T}{2} \operatorname{sinc}\left(\frac{fT}{2}\right) e^{j\frac{\pi T f}{2}} \right]$$

where * denotes the convolution, in this case in the frequency domain.

Now, assuming f_0 to be much greater than the swept bandwidth, Δf , so that the negative frequency contributions are negligible in the positive region, and considering only the magnitude for the positive frequencies:

$$|s(f)| = \left| \sum_{n=-\infty}^{\infty} \sum_{K=-\infty}^{\infty} J_n(\beta_1) J_K(\beta_2) \{ \delta[f - (f_0 + 0.43D_f + nf_{m1} + Kf_{m2})] \right. \\ \left. * \delta(f - \frac{1}{2T}) * \frac{T}{2} \text{sinc}(\frac{fT}{2}) \right|$$

Using Fourier transform properties, the magnitude of $s(f)$ can be expressed as:

$$|s(f)| = \left| \sum_{n=-\infty}^{\infty} \sum_{K=-\infty}^{\infty} J_n(\beta_1) J_K(\beta_2) \frac{T}{2} \text{sinc} \left[\frac{(f-f_0 - \frac{1}{2T} - 0.43D_f - nf_{m1} - Kf_{m2})T}{2} \right] \right|$$

where D_f is a constant used to determine the swept spectrum bandwidth, $\Delta\omega$. Figure 14 shows a plot of the magnitude of the spectrum, $s(f)$, obtained by utilizing the FFT (fast Fourier transform) and plotting capabilities of SAWCAD.

For a matched filter pulse-compression system, the matched filter impulse response can be written directly as:

$$h(t) = \cos \left\{ \omega_0 \left(\frac{T}{2} - t \right) + 0.43D_f \left(\frac{T}{2} - t \right) + \frac{0.5T}{2\pi} \sin \left(\frac{2\pi(T/2 - t)}{T} \right) \right. \\ \left. + \frac{0.07T}{4\pi} \sin \left(\frac{4\pi(T/2 - t)}{T} \right) \right\} \cdot \cos \left(\frac{2\pi(t + T/4)}{T} \right) \cdot \text{rect} \left(\frac{t + T/4}{T/2} \right)$$

A plot of the matched filter impulse response is shown in Figure 15.

The desired output, the auto-correlation function $g(t)$, can be obtained by several different methods. The first, but most difficult, method is to actually perform the convolution and obtain the auto-correlation function directly. In which case:

$$g(t) = s(t) * h(t)$$

Since for a matched filter,

$$h(t) = s(\tau - t)$$

then

$$g(t) = s(t) * s(\tau - t)$$

A second method of obtaining the desired output is to multiply the signal spectrum and the matched filter spectrum to obtain an output spectrum, $G(\omega)$. Then, the inverse Fourier transform will yield the desired output, $g(t)$. In equation form, it looks like:

$$G(\omega) = S(\omega) \cdot H(\omega)$$

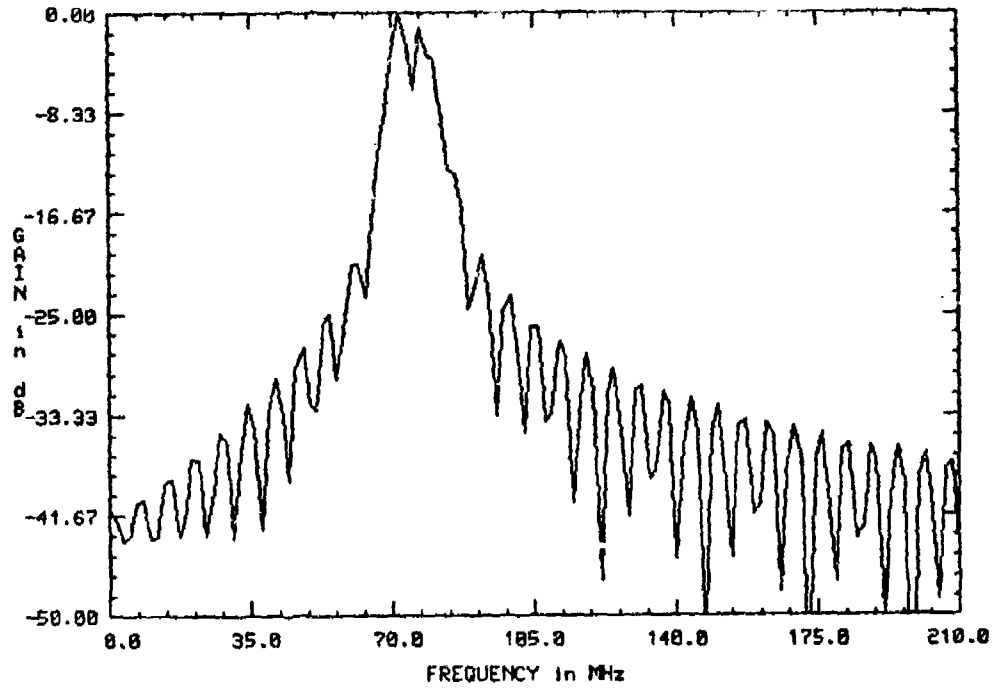


Figure 14. Plot of New Non-Linear FM Spectrum.

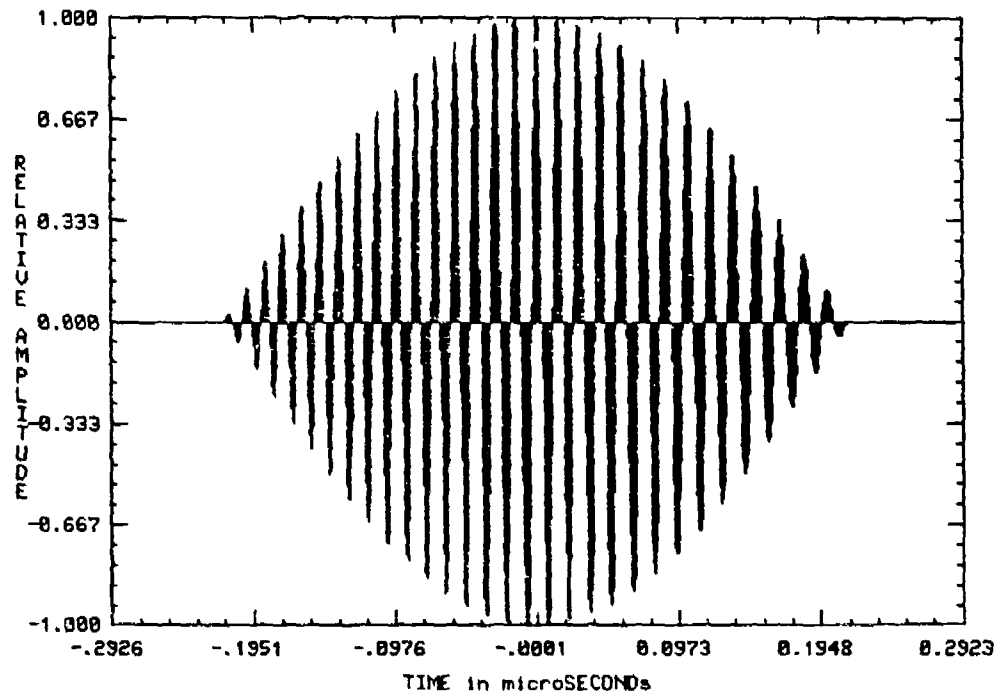


Figure 15. New Non-Linear FM Matched Filter Impulse Response.

and then

$$g(t) = \mathcal{F}^{-1} \{G(\omega)\}$$

This process was accomplished on SAWCAD, and $G(\omega)$ is shown plotted in Figure 16 and $g(t)$ in Figure 17. A quick comparison of this auto-correlation function with that of the linear FM will show the reduction in sidelobe levels. A complete and thorough comparison will be accomplished in a later section of this paper.

Comparison of Properties with Linear and Non-Linear FM Systems

In any radar system, there are, in general, three performance parameters that are of prime importance. They are:

1. Bandwidth - Range resolution is determined by the frequency structure or spectrum of the signal. For a given spectral shape, range resolution is proportional to $1/F$ where the bandwidth of the signal is F cycles.
2. Time Duration - Velocity (that is, the radial component of target velocity) resolution is determined by the time structure or envelope of the signal. For a given envelope shape, velocity resolution is proportional to $1/T$ cycles, where the time duration of the signal is T seconds. Finest velocity resolution is obtained with a signal which has a rectangular envelope.
3. Received Signal, $g(t)$, Energy - Target detectability is determined by the ratio of received signal energy to receiver noise power, S/N ratio.

Of course, all three of these parameters are related to each other through time-frequency domain transforms.

In this section, primary emphasis will be given to comparing the properties of the matched filter output (auto-correlation function)

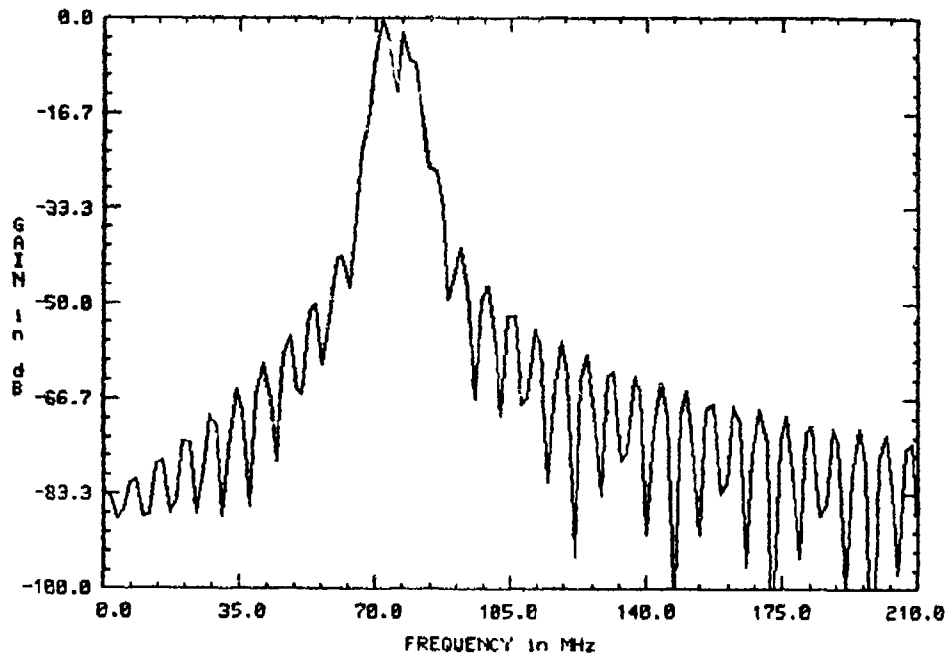


Figure 16. New Non-Linear FM Matched Filter Output Spectrum.

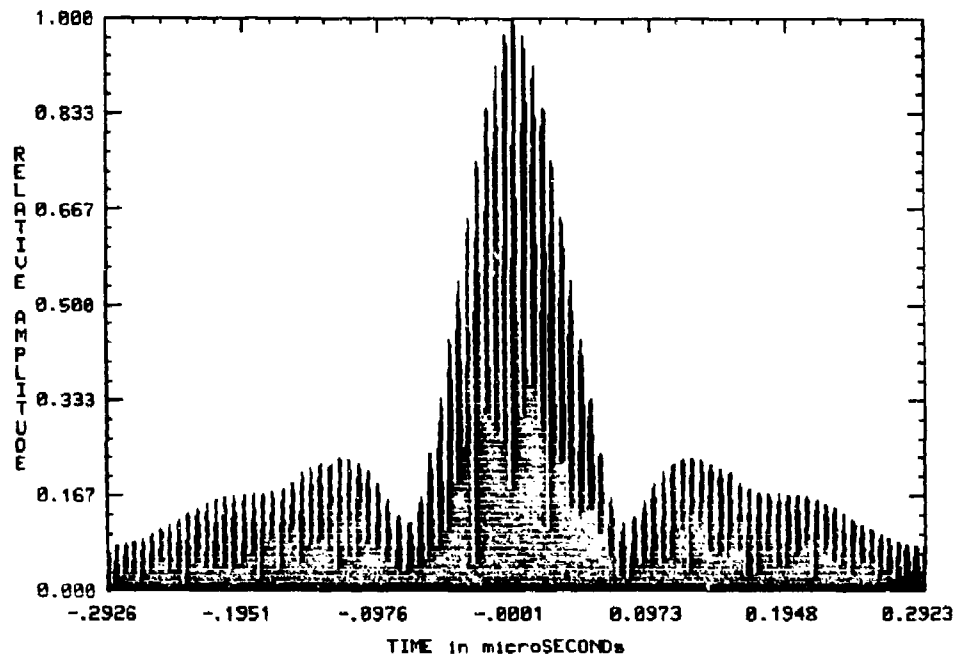


Figure 17. New Non-Linear FM Auto-Correlation.

of linear and new non-linear FM pulse-compression systems. The auto-correlation function can be thought of as a summary of the three parameters listed previously. In all data, it is assumed that the input to the matched filter, $r(t)$, is ideal, and contains no Doppler frequency shifts.

In this first comparison, the auto-correlation function of the new non-linear FM, Figure 18, is compared to the auto-correlation function of linear FM, Figure 19. Table 2 lists the characteristics of each system for a time-bandwidth product of 4.8.

TABLE 2
CHARACTERISTICS OF NEW NON-LINEAR FM
AND LINEAR FM WITH A TIME-BANDWIDTH PRODUCT OF 4.8

	NEW NON-LINEAR FM	LINEAR FM
Center Frequency, f_0 (MHz)	70	70
Pulse Length, τ (micro sec)	.42857	.42857
Bandwidth, Δf (MHz)	11.14	11.14
Time-Bandwidth Product, $\tau\Delta f$	4.8	4.8
Time Sidelobe Level (dB)	-12.623	-23.5
(3 dB) Compressed Pulse Width, T (micro sec)	.055	.078
Actual Compression Rate, τ/T	7.8	5.5

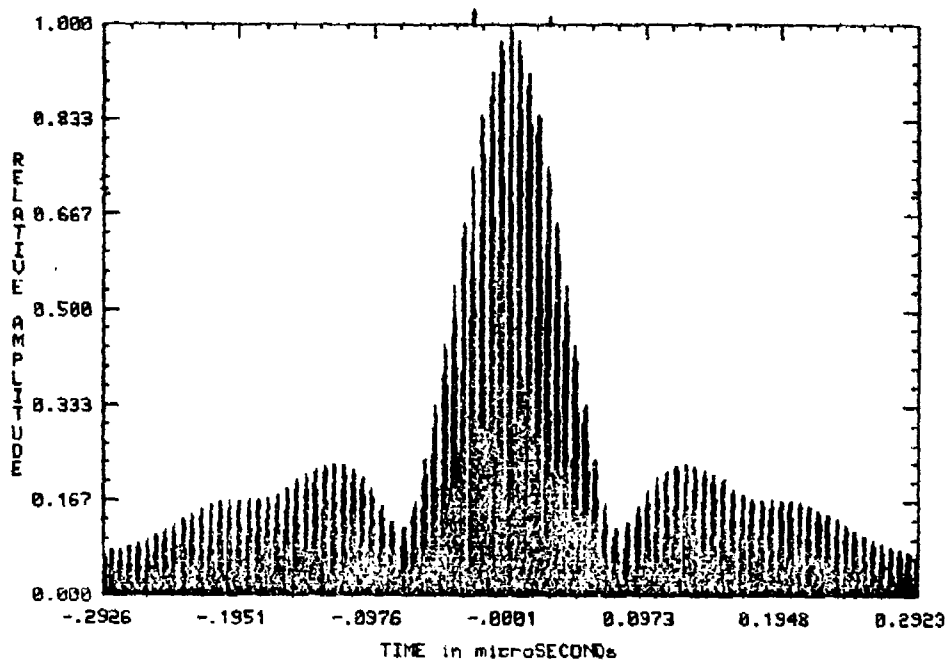


Figure 18. Plot of Auto-Correlation Function for New Non-Linear FM, $\tau\Delta f = 4.8$.

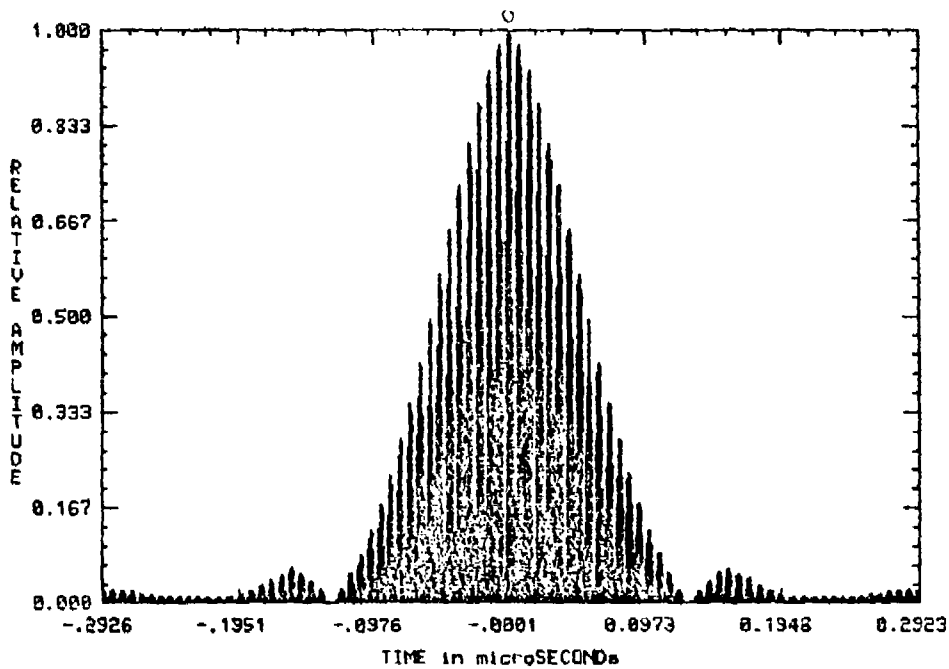


Figure 19. Plot of Auto-Correlation Function for Linear FM, $\tau\Delta f = 4.8$.

A brief review of the characteristics listed in Table 2 shows that the new non-linear FM has higher sidelobes, -12.6 dB, than the linear FM, -23 dB. It is obvious that at this particular time-bandwidth product, the linear FM would still be better. Also of interest is the fact that the new non-linear FM achieved an actual compression ratio of 7.8 as compared to 5.5 for the linear FM. This could possibly be exploited to yield higher range resolution.

In this next comparison, a cosine window function has been added to both the new non-linear, Figure 20, and the linear FM, Figure 21, signals and matched filter. Table 3 summarizes the characteristics of each system for a time-bandwidth product of 4.8.

TABLE 3

CHARACTERISTICS OF NEW NON-LINEAR FM AND LINEAR FM WITH
A TIME-BANDWIDTH PRODUCT OF 4.8 AND A COSINE WINDOW ON ALL SIGNALS

	NEW NON-LINEAR FM	LINEAR FM
Center Frequency, f_0 (MHz)	70	70
Pulse Length, τ (micro sec)	.42857	.42857
Bandwidth, Δf (MHz)	11.14	11.14
Time-Bandwidth Product, $\tau \Delta f$	4.8	4.8
Time Sidelobe Level (dB)	\approx -20	\approx -17.5
(3 dB) Compressed Pulse Width, T (micro sec)	.08385	.11310
Actual Compression Ratio, τ/T	5.11	3.79

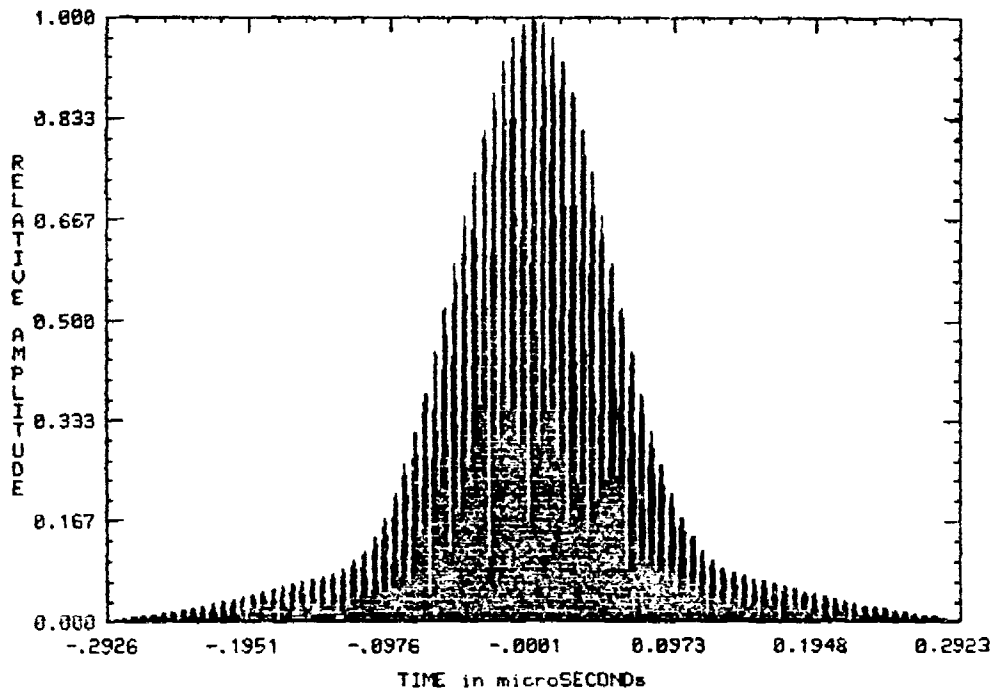


Figure 20. Plot of Auto-Correlation Function for New Non-Linear FM with Cosine Window, $\tau\Delta f = 4.8$.

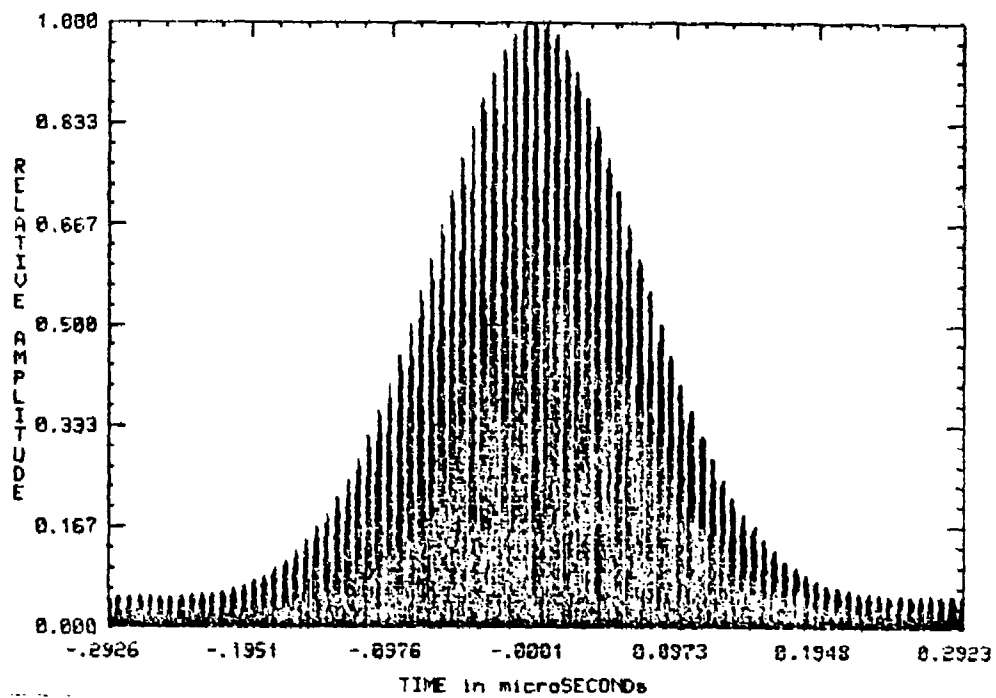


Figure 21. Plot of Auto-Correlation Function for Linear FM with Cosine Window, $\tau\Delta f = 4.8$.

The addition of the cosine window has the effect of reducing the auto-correlation time sidelobes, but at the same time increasing the compressed pulse width. The window has caused these sidelobes to be masked and, therefore, not detectable. A comparison of the characteristics listed in Table 3 shows that the new non-linear FM now has lower sidelobes, -20 dB, than the linear FM, -17.5 dB. Also, the new non-linear FM achieved an actual compression ratio of 5.11 as compared to 3.8 for the linear FM. In this case, the new non-linear FM would perform better in a situation where range resolution is of primary concern.

Design Procedures and Considerations

The complete design of any surface wave device has to take into account the input signal, in both the time and frequency domains, and also the various second-order effects in order to satisfy demanding system requirements. The general design considerations for dispersive devices (both linear and non-linear FM are dispersive) has been examined (Ristic 1983) and will be reviewed here.

The first step in designing a sampled SAW device is to determine the electrode (finger) placement. For dispersive devices, this placement must be such that the waveform is real. This can be accomplished by determining when the signal phase is either 0 or π , as illustrated in Figure 22 (Ristic 1983).

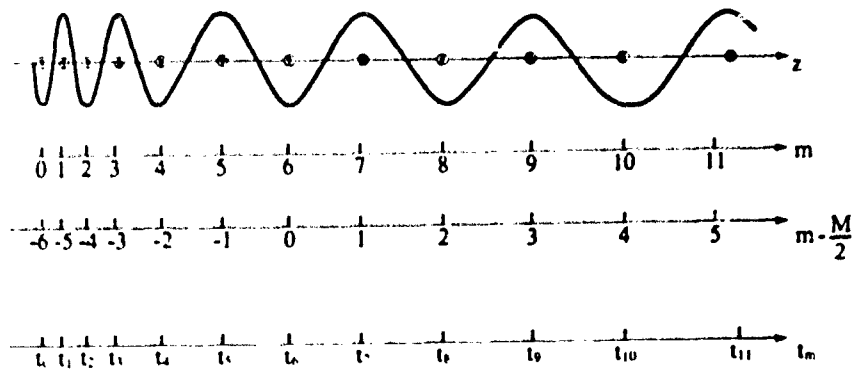


Figure 22. Determining Electrode (Finger) Placement at Time t_m .

The sample time, t_m , is determined by solving the equation: $\sin \phi (t) = 0$. As an example, for linear FM:

$$\phi (t) = 2\pi (f_0 t + \frac{\Delta f}{2T} t^2)$$

Now solving $\sin \phi (t) = 0$ yields:

$$\phi (t_m) = m\pi + c$$

where m is the sample number and c is an unknown constant. The constant c is determined to put the time t_m at the origin of the

time scale, $t_m = 0$. If M is the total number of samples (electrodes) desired, then:

$$\phi(t_m) = 2\pi \left(f_0 t_m + \frac{\Delta f}{2T} t_m^2 \right) = m\pi + c$$

and

$$2 \left(f_0 t_m + \frac{\Delta f}{2T} t_m^2 \right) = m - \frac{M}{2}$$

Therefore:

$$M = 2 f_0 T + 1$$

Now, solving for t_m :

$$t_m = \frac{f_0 T}{\Delta f} \left\{ -1 + \left[1 - \frac{\Delta f}{f_0^2 T} \left(\frac{M}{2} - m \right) \right]^{1/2} \right\}$$

This now determines the time when the linear FM signal should be sampled to obtain only the real amplitude peaks. This is a form of non-uniform sampling, and is accomplished in the following manner. The signal waveform is sampled according to:

$$h(t) = \cos \phi(t) \sum_m [\delta \phi(t) - m\pi]$$

where $\phi(t) = \omega_0 t + \frac{\Delta \omega}{2T} t^2$.

In order to account for the fact that the major contribution to the spectrum occurs at the lower frequencies, the device will need

to be amplitude apodized inversely with respect to the instantaneous frequency.

In equation form, this looks like:

$$h'(t) = \cos \phi(t) \sum_m \frac{\delta(t - t_m)}{|\phi'(t_m)|}$$

where $\phi'(t_m)$ is the instantaneous frequency at sample time t_m . This can be rewritten as:

$$h'(t) = \sum_m \cos \phi(t_m) \frac{\delta(t - t_m)}{|\phi'(t_m)|}$$

This equation is now in the form of a general relationship that can be used to determine the sample position and amplitude for any dispersive device. It should be noted that the amplitude apodization stated above would yield a constant amplitude signal under conditions in which no other losses are present. However, it has been noted (Ristic 1983) that losses which increase with frequency exist and are predominant in practical devices. Therefore, the required amplitude apodization will be an increasing function of frequency.

In applying the above relationship to the non-linear FM introduced in this paper, it is noted that the equation for t_m is quite complex. As an alternative to the equation, the sample times (t_m) can be located by detecting the zero-crossing times and then sampling at the midpoint between each pair of zero-crossing times. This can be accomplished by sampling the signal at a very high rate

to locate the zero-crossings. The above procedure will establish sampling times and amplitudes. It should also be noted that when the electrodes are laid down on the substrate, it is desirable to maintain a 50% duty cycle. That is, to maintain equal electrode and spacing widths. This will require that the finger width be reduced proportionally to the increase in frequency. A sketch depicting this effect is shown in Figure 23.

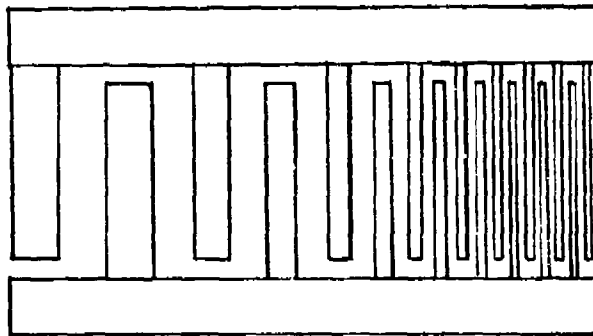


Figure 23. Sketch of Electrode (Finger) Placement for New Non-Linear FM.

Some second-order effects have been considered in the design of a dispersive SAW device (Jones et al. 1972) and will be reviewed here. Basically, choice of substrate, beam spreading, finger placement accuracy, weighting to reduce sidelobes, cascading, multiple transit reflections, temperature effects and input admittance and matching must all be considered when actually building the device. The majority of these secondary considerations have already been incorporated into SAWCAD.

In an actual implementation of a dispersive device, it will be necessary to include compensation to account for the fact that input admittance varies with frequency. This compensation will be in the form of amplitude weighting proportional to $1/f$. Figure 24 depicts the way the transducer fingers will appear. Before this device can be implemented using SAWCAD, it will be necessary to modify SAWCAD STRUCTURE program to enable it to handle dispersive devices.

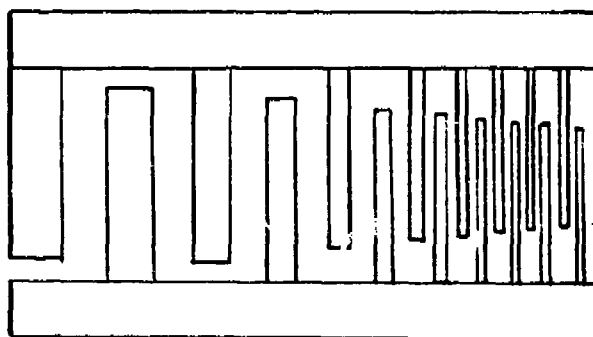


Figure 24. Sketch Showing Finger Placement and Amplitude Weighting.

CHAPTER IV

CONCLUSION AND SUMMARY

Matched filtering and pulse-compression concepts have been reviewed in the context of radar signal processing. The application of these concepts to linear and non-linear FM have been examined with the primary emphasis being given to the auto-correlation output function. It was shown that for most applications, linear FM provides the best overall performance. One limitation that exists in linear FM is that the auto-correlation sidelobe level is limited to -23 dB for high time-bandwidth products.

Non-linear FM pulse-compression is one way to exceed this sidelobe limitation. Several successful versions of non-linear FM were reviewed. The major shortcoming of these implementations is that the design procedure is iterative.

A new non-linear FM pulse-compression technique was introduced and evaluated for implementation on a surface acoustic wave (SAW) device using SAWCAD. It was shown that for some applications, specifically low time-bandwidth product cases, this non-linear FM could possibly perform better than linear FM.

In the final section, design considerations are discussed. The major design consideration, finger (electrode) placement, has been discussed. The conclusion being that finger placement will have to

be accomplished by determining the zero-crossings and sampling at the midpoint between respective zero-crossings. It was also shown that amplitude weighting will be necessary to counter the effects of increased admittance with increasing frequencies.

In final conclusion, the implementation of this new non-linear FM using SAWCAD will require that SAWCAD be modified to handle any dispersive device design.

REFERENCES

- Barton, David K. Radar System Analysis. Dedham, MA: Arctech House, Inc., 1976.
- Bernfield, M.; Cook, C.E.; Paslillo, J.; and Palmieri, C.A. "Matched Filtering, Pulse-Compression and Waveform Design." Microwave Journal 7 (October 1964): 57-64.
- Cook, Charles E. "Pulse Compression - Key to More Efficient Radar Transmission." Proceedings, Institute of Radio Engineering 48 (March 1960): 310-316.
- Cook, Charles E., and Bernfield, Marvin. Radar Signals - An Introduction to Theory and Application. New York: Academic Press, 1967.
- Gradshteyn, I.S., and Ryzhik, I.M. Table of Integrals, Series and Products. New York: Academic Press, 1980.
- Jones, W.S.; Kempf, R.A.; and Hartmann, C.S. "Practical Surface Wave Chirp Filters for Modern Radar Systems." Microwave Journal 15 (May 1972): 43-50.
- Klauder, J.R.; Price, A.C.; Darlington, S.; and Albersheim, W.J. "Theory and Design of Chirp Radars." Bell System Technical Journal 39, 4 (July 1960): 745-808.
- Malocha, D.C., and Richie, S.M. "Computer Aided Design of Surface Acoustic Wave Bi-directional Transducers." Final Report to Texas Instruments, March 1984.
- Millett, Robert E. "A Matched-Filter Pulse-Compression System Using a Non-Linear FM Waveform." IEEE Transactions on Aerospace and Electronic Systems 6 (January 1970): 73-78.
- Ramp, H.O., and Wingrove, E.R. "Principles of Pulse-Compression." Transactions IRE 5, 2 (April 1961): 109-116.
- Ristic, Velimir M. Principles of Acoustic Devices. New York: John Wiley and Sons, Inc., 1983.
- Watson, G.N. Theory of Bessel Functions. Cambridge, MA: Cambridge University Press, 1966.